Chinese Journal of Aeronautics, 2013,26(1): 242–248

Chinese Society of Aeronautics and Astronautics
& Beihang University

Chinese Journal of Aeronautics

cja@buaa.edu.cn
www.sciencedirect.com

Effects of geometrical parameters on wrinkling of thin-walled rectangular aluminum alloy wave-guide tubes in rotary-draw bending

Tian Shan, Liu Yuli *, Yang He

State Key Laboratory of Solidification Processing, Northwestern Polytechnical University, Xi'an 710072, China

Received 31 August 2011; revised 6 December 2011; accepted 9 January 2012
Available online 16 January 2013

KEYWORDS

Geometrical parameters;
Inner flange wrinkling;
Side wrinkling;
Simulation;
Thin-walled rectangular wave-guide tube;
Rotary-draw bending

Abstract Inner flange and side wrinkling often occur in rotary-draw bending process of rectangular aluminum alloy wave-guide tubes, and the distribution and magnitude of wrinkling is related to geometrical parameters of the tubes. In order to study the effects of geometrical parameters on wrinkling of rectangular wave-guide tubes, a 3D-FE model for rotary-draw bending processes of thin-walled rectangular aluminum alloy wave-guide tubes was built based on the platform of ABAQUS/Explicit, and its reliability was validated by experiments. Simulation and analysis of the influence laws of geometrical parameters on the wave heights of inner flange and side wrinkling were then carried out. The results show that inner flange wrinkling is the main wrinkling way to rectangular wave-guide tubes in rotary-draw bending processes, but side wrinkling cannot be neglected because side wrinkling is 2/3 of inner flange wrinkling when b and h are smaller. Inner flange and side wrinkling increase with increasing b and h; the influence of b on side wrinkling is larger than that of h, while both b and h affect inner flange wrinkling greatly. Inner flange and side wrinkling decrease with increasing R/h; the influence of h on inner flange and side wrinkling is larger than that of R.

1. Introduction

Thin-walled rectangular aluminum wave-guide tubes have been widely used in radar, communication, aerospace, and other fields, and rotary-draw bending is their main forming method. However, rotary-draw bending process is a complex forming process with many dies restriction, during which the tube forming quality can be seriously affected by wrinkling, cross-section distortion, etc. The wrinkling of a rectangular wave-guide tube in rotary-draw bending occurs not only in the compressive stress zone of its inner flange, but also in its side web because of uneven stress distribution. Many different cross-section dimensions of rectangular wave-guide tubes have been used in radar systems for the requirements of different transmission wavelengths, and there are also many different relative bending radii of rectangular wave-guide tubes for the requirements of different space layouts. The wrinkling wave height and distribution in inner flange and side web vary with different cross-section dimensions and bending radii of

* Corresponding author. Tel.: +86 29 88460212 803.
E-mail address: lyl@nwpu.edu.cn (Y. Liu).

Peer review under responsibility of Editorial Committe of CJA.

Production and hosting by Elsevier

1000-9361 © 2013 CSAA & BUAA. Production and hosting by Elsevier Ltd. Open access under CC BY-NC-ND license.
http://dx.doi.org/10.1016/j.cja.2012.12.003

rectangular tubes. Therefore, it is useful to study the characteristics of wrinkling as tube geometrical parameters change.

In recent years, a lot of research on inner flange and side wrinkling of rectangular tubes in bending processes has been carried out home and abroad. Zarei and Kröger[1] studied the hit bending behavior of square aluminum tubes hollow or filled with bubble using experiment and numerical simulation method, and found that there was one wrinkle appearing in the compressive stress zone of the inner flange and two wrinkles in the side web. Corona and Vaze[2,3] studied the pure bending of rectangular section profiles by experiment, and proposed that the combined action of inner flange and side wrinkling led to the collapse of rectangular tubes. Okude et al.[4] studied wrinkling limit improvement of aluminum square tubes in large bending radius during draw bending process. Jia and Gao[5] studied the pressure bending of hollow aluminum profiles for automobile frames, and pointed out that inner flange wrinkling of profiles was similar to the ends pressure instability of thin-walled shells. The wrinkling was not only related to the magnitude of compressive stress, but also to the ratio of the thickness to the width of profile. The smaller the ratio was, the more easily the wrinkling occurred. The profile's ability to resist wrinkling could be improved by increasing the thickness of inner flange. Theoretical analysis, numerical simulation and experimental method are used to study wrinkling of rectangular tubes in draw bending, pressure bending, and rotary-draw bending and their results showed that wrinkling and collapse could be eliminated effectively by using inner mandrel.[6–10] The ratio of width to thickness and material strain hardening were the main reasons of inner flange wrinkling; after the occurrence of wrinkling, the wrinkling wave deformation in inner compressive stress zone developed faster to the even deformation in outer tensile stress zone. Studies in these literatures do not give the influence of geometrical parameters on inner flange and side wrinkling systematically. The effects of tube diameters and bending radii on forming quality of round tubes are studied in Refs.[11–13], which provided guidance to the research of this paper. Zhao et al.[14,15] mainly studied the effects of process parameters on wrinkling of rectangular wave-guide tubes in rotary-draw bending based on the platform ABAQUS/Explicit, but only one size of tube was studied and the wrinkling variation characteristics for different geometrical parameters were not researched. However, different cross-section dimensions and different relative bending radii for rectangular wave-guide tubes are needed in radar system. Therefore, the influence laws of the ratio of width to height (b/h) and neutral line relative bending radius (R/h) on wrinkling were researched using numerical simulation method.

2. Description of wrinkling wave height

2.1. Description of wave height of inner flange wrinkling

Fig. 1 shows the schematic diagram of inner flange wrinkling. The wave height of inner flange wrinkling can be expressed as follows:

$$\Delta h_i = h - \sqrt{|A_iB_i|^2 - |A_iC_i|^2} \quad (i = 0, 1, \ldots, j) \tag{1}$$

where h is the original height of a rectangular wave-guide tube; A_i and B_i are the center node and the node in outer edge of a cross section after bending respectively; A_iC_i is perpendicular to B_iC_i at C_i; and j is the end grid node in bending part. Thus the wave height of inner flange wrinkling is defined as:

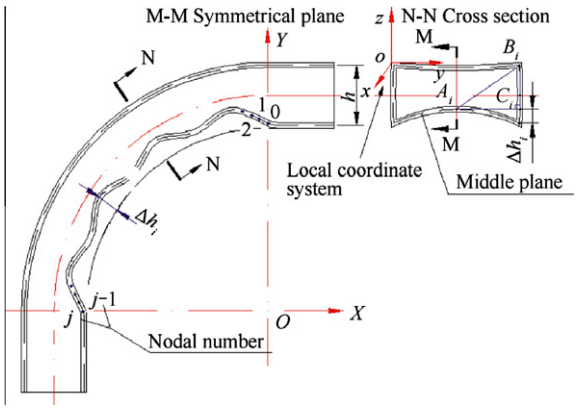

Fig. 1 Schematic diagram of inner flange wrinkling.

$$\Delta h_{\max} = \max\{|\Delta h_i|\} \quad (i = 0, 1, \ldots, j) \tag{2}$$

2.2. Description of wave height of side wrinkling

Fig. 2 shows the schematic diagram of side wrinkling.

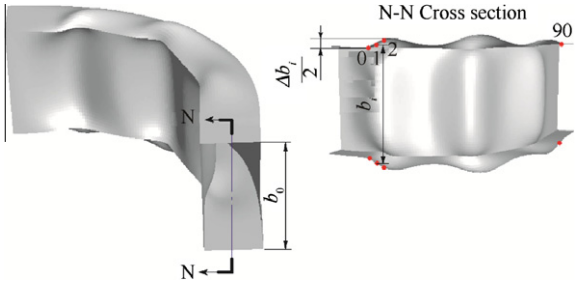

Fig. 2 Schematic diagram of side wrinkling.

From Ref. [16], it can be counted that the maximum wave height of side wrinkling appears in the outer edge of the tube, so the side wrinkling wave height can be expressed as:

$$\Delta b_i = (b - b_i)/2 \quad (i = 0, 1, \ldots, j) \tag{3}$$

where b is the original tube width; b_i the width of the outer edge of a cross section after bending. Thus the wave height of side wrinkling $\Delta b_{\max}$ is defined as:

$$\Delta b_{\max} = \max\{|\Delta b_i|\} \quad (i = 0, 1, \ldots, j) \tag{4}$$

3. FE model and verification of its reliability

3.1. FE model

3.1.1. Material model

Aluminum alloy 3A21 (T4) of extruded rectangular tubes was adopted in numerical simulation, and its mechanical properties were obtained by tensile tests. The specimens for tensile tests were obtained along the length direction of a thin-walled rectangular tube with a width of 24.86 mm, as shown in Fig. 3.The geometry size of the specimen is shown in Fig. 4.

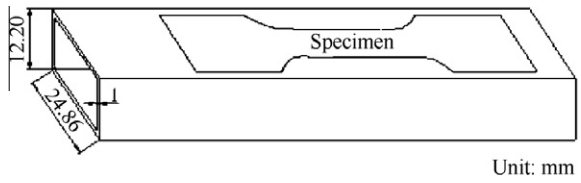

Fig. 3 Specimen for tensile tests.

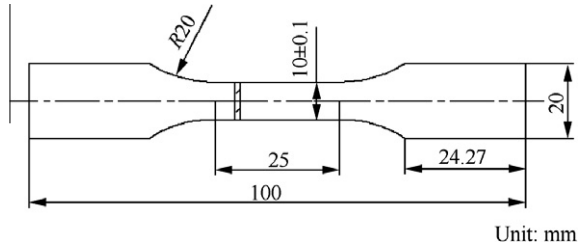

Fig. 4 Geometry size of tensile test specimens.

The stress–strain curve obtained from tensile tests is shown in Fig. 5, and can be expressed in Eq. (5). The basic material parameters are shown in Table 1.

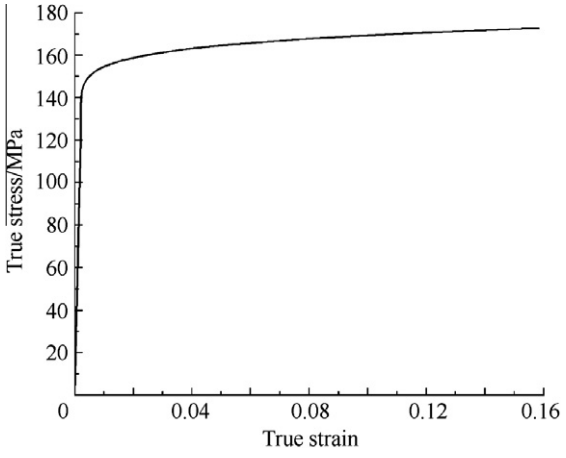

Fig. 5 True stress–strain curve of 3A21 rectangular tubes.

Table 1 Material parameters of 3A21 rectangular tubes.

E (GPa)	ν	$\sigma_{0.2}$ (MPa)	σ_b (MPa)	δ (%)	Hardening index n	Stress intensity factor K (MPa)
60.2	0.33	121.45	151.68	19	0.145	67.8

$$\begin{cases} \bar{\sigma} = 60.2 \times 10^3 \times \bar{\varepsilon} & (0 \leqslant \bar{\varepsilon} \leqslant 0.002) \\ \bar{\sigma} = 121 + 67.8 \times (\bar{\varepsilon} - 0.002)^{0.145} & (\bar{\varepsilon} > 0.002) \end{cases} \quad (5)$$

3.1.2. Friction model and coefficient

Rotary-draw bending of thin-wall rectangular wave-guide tubes is a cold forming process, so the classic Coulomb friction model was chosen to describe friction between a tube and dies. The friction coefficients adopted are shown in Table 2.[16]

Table 2 Friction coefficient between rectangular tubes and dies.

Contact pairs	Friction coefficient
Bend die-tube	0.3
Pressure die-tube	0.3
Clamp die-tube	0.7
Insert die-tube	0.7
Wiper die-tube	0.14
Mandrel-tube	0.1
Core-tube	0.06

3.1.3. Element type and number

The linear reduction integration doubly curved thin shell element with four nodes (S4R) was selected to describe the tubes; the dies were defined as a 3D bilinear rigid quadrilateral discrete rigid element with four nodes (R3D4).

For a tube of $24.86 \times 12.2 \times 1$ mm with its length 200 mm, there are 27,300 elements for this tube, 792 elements for bend die, 480 elements for pressure die, 1544 elements for clamp die, 324 elements for wiper die, 1848 elements for mandrel, and 1590 elements for 3 cores.

Based on the above conditions and the platform of ABAQUS/Explicit, a 3D-FE model for rotary-draw bending process of thin-walled rectangular aluminum-alloy tubes was built, as shown in Fig. 6.

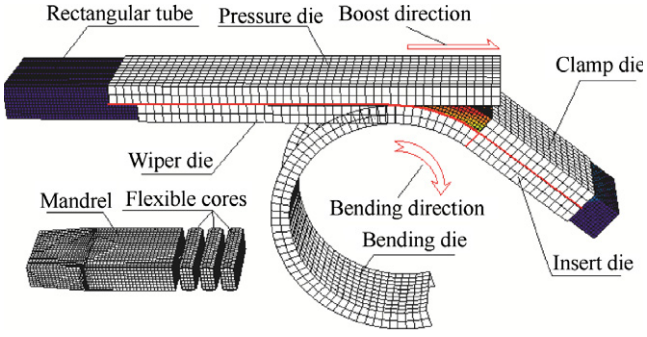

Fig. 6 The meshed 3D-FE model for rotary-draw bending process of rectangular wave-guide tubes.

3.2. Validation of the model

To verify the reliability of the FE model, the experiment for rotary-draw bending process of 3A21 aluminum-alloy rectangular wave-guide tubes was carried out by using PLC controlling hydraulic tube bending machine W27YPC-63.

The dimensions of the tube were $24.86 \times 12.2 \times 1$ mm its length 200 mm, the bending angle 90°, the bending radius 40 mm, the bending velocity 0.5 rad/s, the boost velocity 23.5 mm/s, the clearance between the mandrel and the tube, 0.1 mm, and between other dies and the tube 0. The bending die, pressure die, wiper die, mandrel, cores, and the inner wall of the tube were lubricated by a certain type of aviation lubricating oil. It was dry friction between the clamp die and the outer wall of the tube.

Fig. 7 shows the qualitative comparison of experimental and simulation results of tube bent parts. It can be seen that the agreement between experimental and simulation results is reasonably good. In order to further verify the reliability of the model, a quantitative comparison of the wave height of inner flange wrinkling was carried out, as shown in Fig. 8. From the figure, the wrinkling wave distribution of simulation results is similar to that of the experiments, and the maximum error between experimental and simulation results is less than 5%. Therefore, the results obtained by the model are reliable.

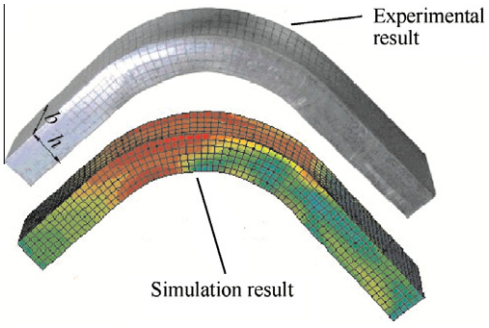

Fig. 7 Qualitative comparison of experimental and simulation result of tube bent parts.

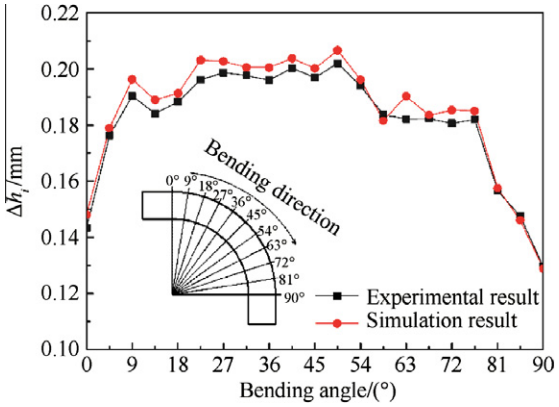

Fig. 8 Quantitative comparison of experimental and simulation results of inner flange wrinkling wave height.

4. Simulation results and discussion

4.1. Effects of relative width b/h on inner flange wrinkling Δh_{max} and side wrinkling Δb_{max}

(1) Retain $h = 20$ mm unchanged, change b, and select $b/h = \{0.5, 0.8, 1.0, 1.2, 1.5, 2.0\}$, that is, the section dimension of rectangular tubes changes from $b < h$ to $b = h$ (square section) and to $b > h$. The relative bending radius $R/h = 3$ (R is the bending radius).

Fig. 9 shows the influence of relative width b/h ($h = 20$ mm) on inner flange wrinkling Δh_{max} and side wrinkling Δb_{max}. It can be seen that Δh_{max} and Δb_{max} increase with increasing b/h. The reasons are that: (1) webs and flanges of rectangular wave-guide tubes restrict one another in

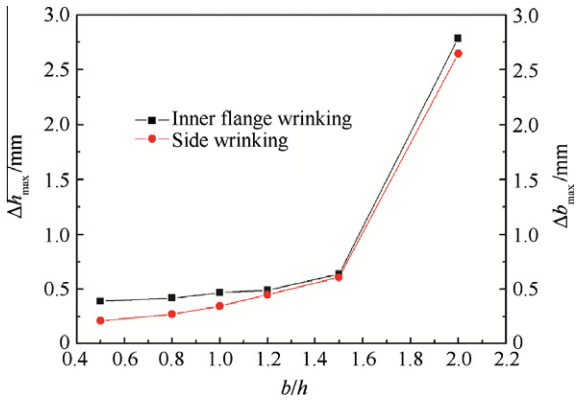

Fig. 9 Δh_{max} and Δb_{max} vs. relative width (b/h) ($h = 20$ mm).

rotary-draw bending process, and the support effect of webs to flanges gets smaller with the increase of b/h or cross-section width b, so wrinkling is more prone to occur with the increase of b/h; (2) while h kept unchanged, the cross-section dimensions become bigger with the increase of b, and the deformation resistance of cross section of the tube gets down, which results in the increase of Δh_{max} and Δb_{max}. Fig. 10 shows the tangential stress distribution of $b = 10$ mm and $b = 40$ mm tubes. It can be seen that the maximum tangential stress is higher and the wrinkles are more obvious when $b = 40$ mm.

It can also be seen from Fig. 9, Δh_{max} is always higher than Δb_{max}. Δh_{max} and Δb_{max} increase gently when $b/h \leqslant 1.5$, and

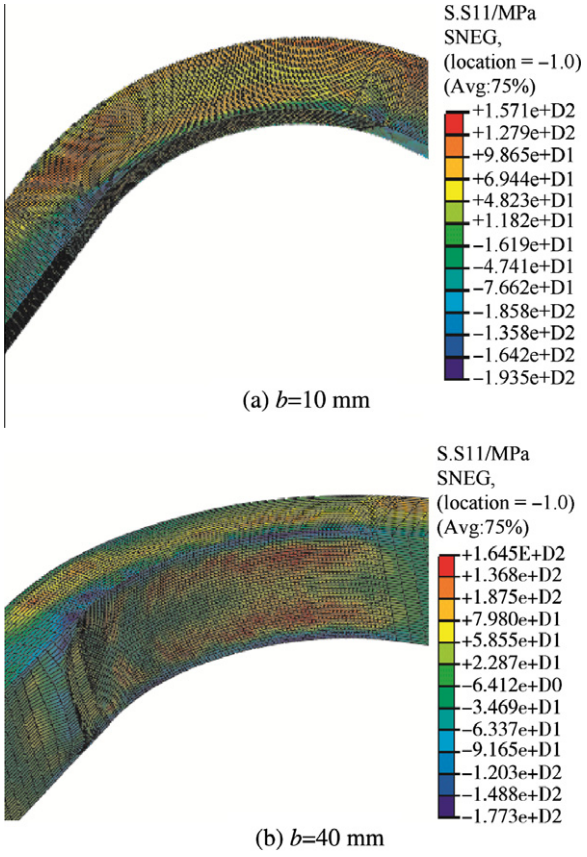

Fig. 10 Tangential stress distribution of different size tubes when $h = 20$ mm.

then rapidly when $b/h > 1.5$, which is because the stiffness of large dimension tubes is poor and wrinkling is easier to occur. That is, the process parameters adopted in this paper are appropriate for the section dimension of $h = 20$ mm and $b < 30$ mm, and the process parameters must be readjusted if the tube section dimension is bigger than this size.

(2) Retain $b = 20$ mm unchanged, change h, and select $b/h = \{0.5, 0.8, 1.0, 1.2, 1.5, 2.0\}$, that is, the section dimension of rectangular tubes is from $b < h$ to $b = h$ (square section) and to $b > h$. The relative bending radius $R/h = 3$.

Fig. 11 shows the influence of relative width b/h ($b = 20$ mm) on inner flange wrinkling Δh_{max} and side wrinkling Δb_{max}. It can be seen that Δh_{max} and Δb_{max} decrease with increasing b/h. The reasons are that: (1) the restrict and support effect of webs to flanges gets smaller with the increase of b/h or decrease of cross-section height h, so wrinkling is more prone to occur with the increase of b/h; (2) while b kept unchanged, the cross-section dimensions become smaller with the decrease of h, and the deformation resistance of cross section of the tube gets up, which results in the decrease of Δh_{max} and Δb_{max}. Because the second reason plays a main role, Δh_{max} and Δb_{max} finally decrease with increasing b/h. Fig. 12 shows the tangential stress distribution of $h = 10$ mm and $h = 40$ mm tubes. It can be seen that the stress in inner flange and outer edge is higher when $h = 40$ mm, which is also the reason why wrinkling is serious when $b/h = 0.5$.

It can also be seen from Fig. 11, Δh_{max} is always higher than Δb_{max}. Δh_{max} and Δb_{max} decrease gently when $b/h \geqslant 0.8$, and then rapidly when $b/h < 0.8$, due to the reason that, as mentioned previously, large dimension tubes are prone to wrinkle. That is, the process parameters adopted in this paper are appropriate for the section dimension of $b = 20$ mm and $h < 25$ mm, and the process parameters must be readjusted if the tube section dimension is bigger than this size.

It can be known from Figs. 9 and 11 comprehensively, Δb_{max} is always smaller than Δh_{max}, that is, inner flange wrinkling is the main wrinkling way for rectangular wave-guide tubes during rotary-draw bending process, but the side wrinkling cannot be ignored because Δb_{max} is 2/3 of Δh_{max} when b and h are smaller ($b \leqslant 20$ mm, $h \leqslant 20$ mm); when b and h get larger ($b > 20$ mm, $h > 20$ mm), Δb_{max} changes differently when b or h changes separately. It can also be seen that both b and h affect Δh_{max} greatly, but the effect of b on Δb_{max} is greater than that of h.

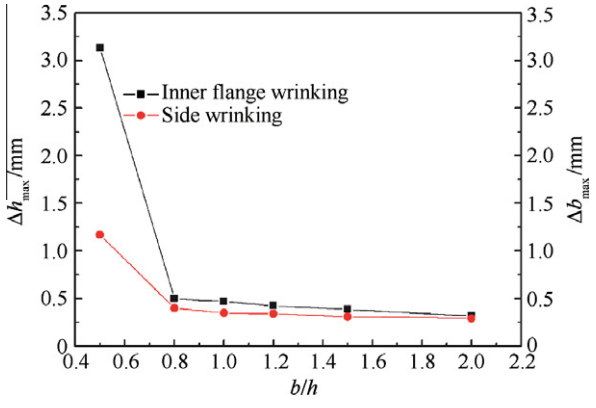

Fig. 11 Δh_{max} and Δb_{max} vs. relative width (b/h) ($b = 20$ mm).

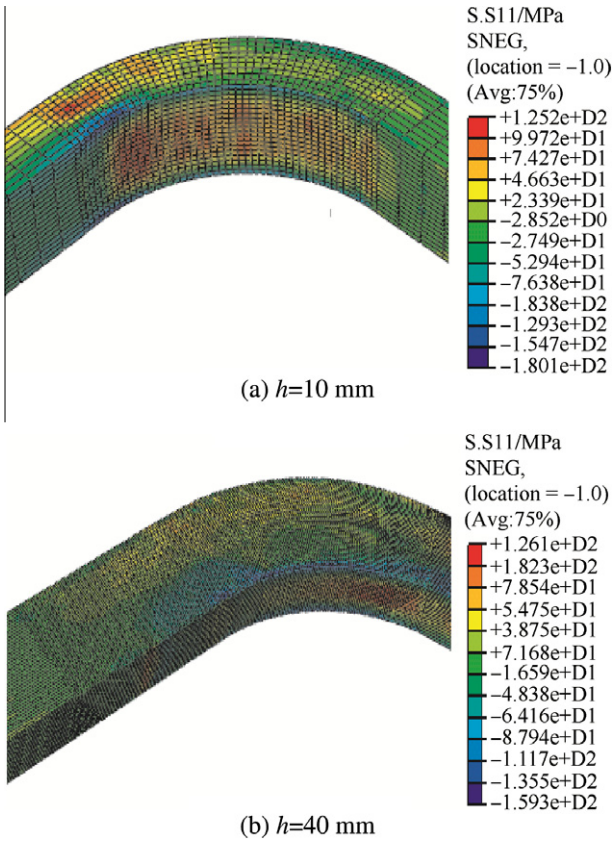

Fig. 12 Tangential stress distribution of different size tubes when $b = 20$ mm.

4.2. Effects of relative bending radius R/h on inner flange wrinkling Δh_{max} and side wrinkling Δb_{max}

(1) Retain $h = 20$ mm unchanged, change R, and select $R/h = \{2.5, 3.0, 3.5, 1.2, 4.0, 5.0\}$.

Figs. 13 and 14 show the influence of relative bending radius R/h ($h = 20$ mm) on inner flange wrinkling Δh_{max} and side wrinkling Δb_{max}, respectively. It can be seen that Δh_{max} and Δb_{max} decrease with increasing R/h. This is because the deformation degree decreases with increasing R/h and induces the tension and compressive stress decrease. When $b/h \geqslant 1$, the support function of two webs to flanges is small and the deformation resistance of rectangular wave-guide tubes is poor, so Δh_{max} and Δb_{max} decrease obviously with increasing R/h; when $b/h < 1$, the deformation resistance is stronger, so Δh_{max} and Δb_{max} decrease gently with increasing R/h. When $R/h \geqslant 3.5$, the curve is nearly unchanged, because the deformation degree is so small that R has little influence on Δh_{max} and Δb_{max}. It can also be known from the two figures that Δh_{max} and Δb_{max} increase with increasing b/h when R/h is unchanged.

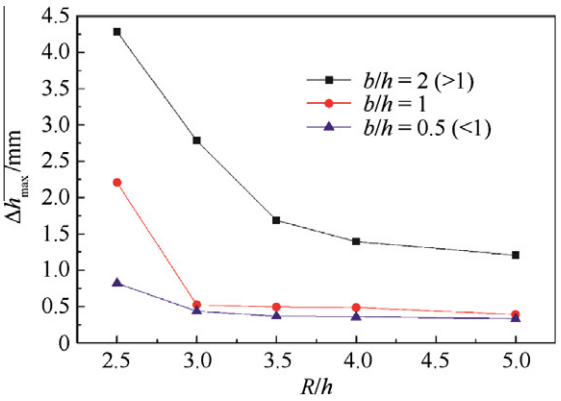

Fig. 13 Δh_{max} vs. relative bending radius (R/h) (h = 20 mm).

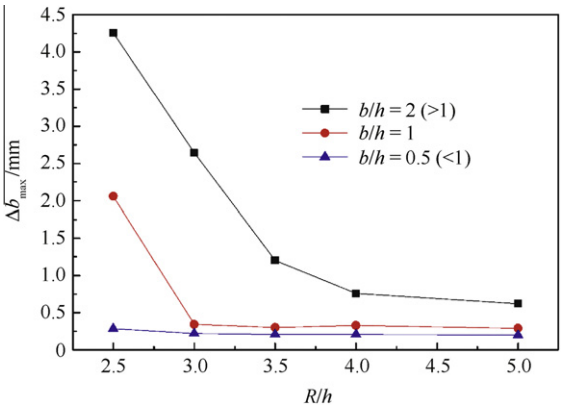

Fig. 14 Δb_{max} vs. relative bending radius (R/h) (h = 20 mm).

(2) Retain R = 60 mm unchanged, change h, and select R/h = {2.5, 3.0, 3.5, 1.2, 4.0, 5.0}.

Figs. 15 and 16 show the influence of relative bending radius R/h (R = 60 mm) on inner flange wrinkling Δh_{max} and side wrinkling Δb_{max}, respectively. It can be seen that Δh_{max} and Δb_{max} decrease with increasing R/h. When $b/h \geqslant 1$, the deformation resistance of rectangular wave-guide tubes increase rapidly with increasing R/h, so Δh_{max} and Δb_{max} decrease obviously; when $b/h < 1$, the cross section dimension is smaller and the deformation resistance is stronger, so Δh_{max} and Δb_{max} decrease gently with increasing R/h. When

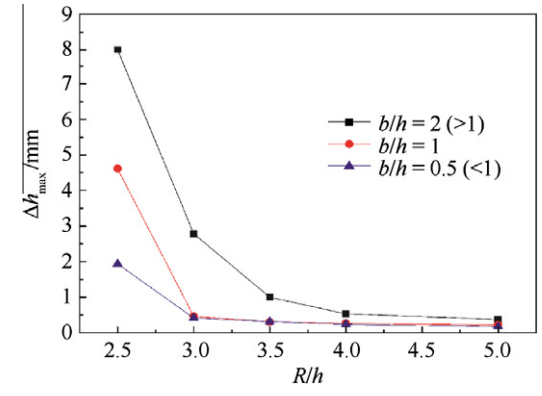

Fig. 15 Δh_{max} vs. relative bending radius (R/h) (R = 60 mm).

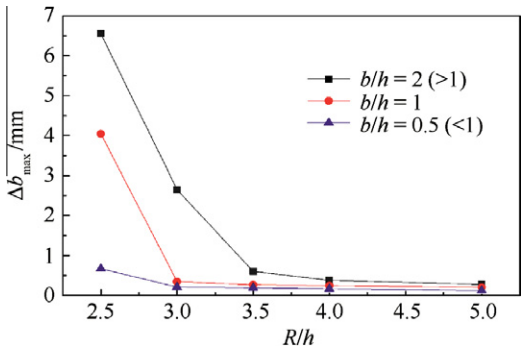

Fig. 16 Δb_{max} vs. relative bending radius (R/h) (R = 60 mm).

$R/h \geqslant 3.5$, the curve is nearly unchanged, because the deformation degree is small. It can also be known from the two figures that Δh_{max} and Δb_{max} increase with increasing b/h when R/h is unchanged.

It can be concluded from Figs. 13–16 that Δb_{max} is always smaller than Δh_{max}. Δh_{max} and Δb_{max} decrease with increasing R/h, but the amount of decrease is different when R or h changes separately. The effect of h on Δh_{max} and Δb_{max} is larger than that of R.

5. Conclusions

(1) Inner flange wrinkling is the main wrinkling way for rectangular wave-guide tubes during rotary-draw bending process, but the side wrinkling cannot be neglected because Δb_{max} is 2/3 of Δh_{max} when b and h are smaller.
(2) Δh_{max} and Δb_{max} increase with increasing b and h; both b and h affect Δh_{max} greatly, but the effect of b on Δb_{max} is larger than that of h.
(3) Δh_{max} and Δb_{max} decrease with increasing R/h; R/h has obvious effect on Δh_{max} and Δb_{max} when $b/h \geqslant 1$ and R/h has little effect on Δh_{max} and Δb_{max} when $b/h < 1$; the effect of h on Δh_{max} and Δb_{max} is larger than that of R.
(4) The process parameters adopted in this paper are appropriate for the section dimension of b = 20 mm and h < 25 mm or h = 20 mm and b < 30 mm. The process parameters must be readjusted if the tube section dimension is bigger than this size.

Acknowledgments

The authors would like to express their appreciation for the financial support of the National Natural Science Foundation of China (No. 50975235 and 50575184) and the 111Project (B08040).

References

1. Zarei HR, Kröger M. Bending behavior of empty and foam-filled beams: Structural optimization. *Int J Impact Eng* 2008;**35**(6):521–9.
2. Corona E, Vaze SP. Buckling of elastic-plastic square tubes under bending. *Int J Mech Sci* 1996;**38**(7):753–75.
3. Vaze SP, Corona E. Degradation and collapse of square tubes under cyclic bending. *Thin-Walled Struct* 1998;**31**(4):325–41.

4. Okude Y, Sakaki S, Yoshihara S. Improving working limit in draw bending process of aluminum square tubes in large bending radius. *Adv Technol Plast* 2008;564–9.
5. Jia LL, Gao JZ. Bending technology of hollow alumal-shape in use for automobile frame. *Met Form Technol* 2000;**18**(6): 34–5 [Chinese].
6. Paulsen F, Welo T. Cross-sectional deformations of rectangular hollow sections in bending: Part II-analytical models. *Int J Mech Sci* 2001;**43**:131–52.
7. Paulsen F, Welo T, Sovik OP. A design method for rectangular hollow sections in bending. *J Mater Process Technol* 2001;**113**(1–3):699–704.
8. Paulsen F, Welo T. Application of numerical simulation in the bending of aluminium-alloy profiles. *J Mater Process Technol* 1996;**58**(2–3):274–85.
9. Welo T, Paulsen F. Local flange buckling and its relation to elastic springback in forming of aluminium extrusions. *J Mater Process Technol* 1996;**60**(1–4):149–54.
10. Paulsen F, Welo T. Cross – sectional deformations of rectangular hollow sections in bending: Part I-experiments. *Int J Mech Sci* 2001;**43**(1):109–29.
11. Yan J, Yang H, Zhan M, Li H. Forming characteristics of Al-alloy large-diameter thin-walled tubes in NC-bending under axial compressive loads. *Chin J Aeronaut* 2010;**23**(4):461–9.
12. Jiang ZQ, Zhan M, Yang H, Xu XD, Li GJ. Deformation behavior of medium-strength TA18 high-pressure tubes during NC bending with different bending radii. *Chin J Aeronaut* 2011;**24**(5):657–64.
13. Li H, Yang H. A study on multi-defect constrained bendability of thin-walled tube NC bending under different clearance. *Chin J Aeronaut* 2011;**24**(1):102–12.
14. Zhao GY, Liu YL, Yang H. Numerical simulation on influence of clearance and friction on wrinkling in bending of aluminum alloy rectangular tubes. *Mater Sci Forum* 2007;**546–549**:833–8.
15. Zhao GY, Liu YL, Yang H. Numerical simulation of influence of mandrel on wrinkling in bending of thin-walled rectangular tube. *China Mechanical Engineering*. 2006;**17**(Suppl 1):35–7, 66 [Chinese].
16. Zhao GY. Study on wrinkling behaviors and; limit during NC rotary-draw bending process of thin-walled rectangular tube dissertation. Xi'an: Northwestern Polytechnical University; 2010 [Chinese].

Tian Shan received her B.S. degree from Northwestern Polytechnical University in 2009, and then became a master student there. Her main research interest is rotary-draw bending process of thin-walled rectangular wave-guide tubes.

Liu Yuli is a professor at Northwestern Polytechnical University. Her main research interests are precision plastic forming and computer simulations.

Yang He is a professor at Northwestern Polytechnical University. He is also the Yangtze River Scholar and the recipient of China National Funds for Distinguished Young Scientists. His main research interests are precision plastic forming and computer simulations.